Anion ordering in spinel-type gallium oxonitride

Teak D. Boyko, Carmen E. Zvoriste, Isabel Kinski, Ralf Riedel, Stefanie Hering, Hubert Huppertz, and Alexander Moewes

Phys. Rev. B **84**, 085203 — Published 19 August 2011

DOI: 10.1103/PhysRevB.84.085203

Anion ordering in spinel-type gallium oxonitride

Teak D. Boyko,[1,*] Carmen E. Zvoriste,[2] Isabel Kinski,[3] Ralf Riedel,[2]
Stefanie Hering,[4] Hubert Huppertz,[4] and Alexander Moewes[1]

[1] *Department of Physics and Engineering Physics, University of Saskatchewan, Saskatoon, Saskatchewan, S7N 5E2, Canada.*
[2] *Fachbereich Material- und Geowissenschaften, Technische Universität Darmstadt, D-64287 Darmstadt, Germany.*
[3] *Fraunhofer Institute for Ceramic Technologies and Systems, D-01277 Dresden, Germany.*
[4] *Department Chemie, Ludwig-Maximilians-Universität München, D-81377 München, Germany.*

(Dated: August 1, 2011)

The specific locations of the anions — nitrogen and oxygen — in the crystallographic sites are not known in the spinel-type gallium oxonitride. We report here on an indirect method for determining the specific location of the light elements, N and O, in a defect spinel-structured gallium oxonitride, $Ga_{2.79}O_{3.05}N_{0.76}$. The locations of elements that are adjacent in the periodic table ($\Delta Z = \pm 1$) are indistinguishable with conventional XRD techniques. However, by examining the local electronic structure we show that the anions are spatially ordered such that, $R\bar{3}m$ (No. 166) is the most appropriate defect free space group. Finally, we have determined experimentally the electronic band gap of $Ga_{2.79}O_{3.05}N_{0.76}$ to be 2.95 ± 0.30, agreeing with our calculated value of 2.79 eV (direct) for Ga_3O_3N using MBJLDA.

I. INTRODUCTION

Over the last decade, spinel-structured nitrides have been an active area of research spurred by the synthesis of the first spinel-structured nitride, silicon nitride (γ-Si_3N_4)[1]. Almost simultaneously, spinel-structured germanium nitride (γ-Ge_3N_4)[2] was synthesized using similar methods. These nitride phases are synthesized in a high pressure (15 GPa) and high temperature (2000 K) environment from their low-pressure trigonal/hexagonal phases (α-Si_3N_4/β-Si_3N_4) via shock synthesis experiments[3] or diamond anvil cell (DAC)[4] and multi-anvil cell (MAC)[5] experiments. Several studies were carried out regarding ternary nitrides/oxonitrides[6–15] in an effort to tailor the highly desirable mechanical and electronic properties associated with spinel nitrides to suit specific applications.

Gallium oxonitride (Ga_3O_3N) with spinel structure was first predicted by Lowther *et. al.*[16], and has since been synthesized recently by several groups[12,14,17]. The large amount of interest in this material is due to the wide spread use of its precursors, w-GaN and β-Ga_2O_3. Furthermore, Ga3O3N is thought to have robust mechanical and chemical properties similar to its binary precursors, and a predicted direct electronic band gap[10–12].

The electronic band gap of a functional material is arguably one of the most important properties. Numerous theoretical studies have focused on the electronic properties and electronic band gaps of compounds with spinel structure[6,7,18]. Spinel-structured nitrides, in comparison to their respective low-pressure phases, exhibit reduced band gaps values that are comparable to the visible spectrum[6,19]. With the knowledge that these cubic crystals with large coordination numbers (CN) have reduced electronic band gaps, research has expanded further into spinel-type oxonitrides in an effort to engineer the band gap value by varying the N/O ratio. Previously, theoretical studies show that gallium oxonitride with ideal structure (Ga_3O_3N) might have a band gap comparable to that of w-GaN or slightly larger[10,12] allowing potentially useful electronic applications. Direct band gap values calculated using the local density approximation (LDA) and generalized gradient approximation (GGA) are 1.72 eV and 1.37 eV, respectively[13]. However, it is well known that LDA and GGA calculations underestimate the band gap[20] and the actual band gap value of Ga_3O_3N may be as large as 4 eV[10]. To date, there are no reports of a measured band gap value for cubic gallium oxonitride.

There are two recent reports on the synthesis of a defect structure gallium oxonitride[12,14]. These studies show that in the gallium oxonitride the octahedral site in the spinel structure is not fully occupied and has inherent octahedral gallium vacancies. The two studies report gallium oxonitride with similar stoichiometry, $Ga_{2.79}\square_{0.21}O_{3.05}N_{0.76}\square_{0.19}$[14] and $Ga_{2.81}O_{3.24}N_{0.64}$[12], where $\square$ indicates cationic and anionic vacancies. The occupation of the cation sites, 2.79/3.00[14] and 2.81/3.00[12], was determined through X-ray Diffraction (XRD) measurements. However, in order to determine the anion occupations, the ratio of N/O was determined with electron micro-probe or electron energy loss spectroscopy measurements, which was used as a fitting parameter. The complete structural picture (including differentiating between the positions of N and O) of spinel-type gallium oxonitride is not well known. The current experimental results show that the $Ga_{2.79}O_{3.05}N_{0.76}$ system crystallizes in the spinel-type structure ($Fd\bar{3}m$ No. 227) with tetrahedrally and octahedrally coordinated gallium cations, while the anions are tetrahedrally coordinated. The site occupation of the cations (Ga Wyckoff sites $8a$ and $16d$) is well known, but the positions of the different anions (N and O) are not distinguishable with XRD and are generalized to a single Wyckoff site, $32e$[14,21]. Determining a complete structural picture of $Ga_{2.79}O_{3.05}N_{0.76}$ is invaluable for under-

standing its electronic and mechanical properties. A better understanding of the crystal structure also facilitates more efficient synthesis methods to produce purer phases with tailored mechanical and electronic properties.

Several theoretical works exist discussing the anion ordering in Ga_3O_3N[10,12]. In one of these studies[12], it was assumed that N and O to retain their F arrangements resulting in three distinct ideal (i.e. defect free with an N:O ratio of 1:3) crystallographic groups: $Imm2$ (no. 44), $Ima2$ (no. 46) and $R\bar{3}m$ (no. 166). DFT calculations based on these structures considering equilibrium energy yielded the $R\bar{3}m$ space group as the likely candidate structure and placing the nitrogen atoms in positions such that they are as far away from other nitrogen atoms as possible minimizes the calculated total energy[10], but an experimental confirmation has not yet been reported. This motivates the use of X-ray Absorption Spectroscopy (XAS) measurements, which are a useful tool to examine the local electronic structure. For example, XAS has been employed to determine the local crystal structure of β-SiAlONs[22]. While this technique does not directly probe the crystal structure, it analyses the local electronic structure and as such provides a way to indirectly determine the local bonding environment. This technique and the results presented here determine a possible local structure and the band gap of spinel-type gallium oxonitride.

II. METHODS

The spinel-type gallium oxonitride sample was synthesized using a multi-anvil device based on a Walker-type module and a 1000-ton press (Voggenreiter, Mainleus, Germany). A mixture of w-GaN (99.9 , Alfa Aesar, Karlsruhe, Germany) and β-Ga_2O_3 (99.9 , Sigma Aldrich, Munich, Germany), with the molar ratio of w-GaN:β-Ga_2O_3 = 6:4, was filled into a hexagonal boron nitride capsule (Henze BNP GmbH, HeBoSint S10, Kempten, Germany) and then placed in a 18 / 11-assembly, which was compressed by eight tungsten carbide cubes (TSM-10 Ceratizit, Reutte, Austria). The peak pressure and temperature values were 5 GPa and 1250 °C. The sample required 15 minutes to heat and was allowed to cool to 800 °C for a duration of 25 minutes after the peak temperature was achieved. The sample was then quenched once the temperature reached 800 °C. Final products were separated from the surrounding crucible and XRD was used for the phase analyses of each sample. The data were collected with a Stoe Stadi P diffractometer using monochromatized Cu Kα ($\lambda = 1.54051$ Å) radiation. The β-Ga_2O_3 in the starting mixtures reacted totally to form the spinel gallium oxonitride and a Rietveld refinement of the powder diffraction pattern showed the presence of the spinel gallium oxonitride ($> 95\%$) next to remaining w-GaN.

The local electronic structure around the anions was probed with a combination of X-ray Emission Spectroscopy (XES) and X-ray Absorption Near Edge Spectroscopy (XANES) measurements. XES and XANES were used to probe both the valence band (VB) and conduction band (CB) in $Ga_{2.79}O_{3.05}N_{0.76}$. The unoccupied and occupied states that were probed with N 1s and O 1s excitations were limited to N and O p-states due to the dipole selection rule ($\Delta\ l = \pm 1$), thereby XES and XANES probe the local partial occupied and unoccupied density of states (LPDOS), respectively.

The XES measurements were performed on beamline 8.0.1 at the Advanced Light Source (Berkeley, CA, USA)[23] and were recorded with the grating spectrometer permanently affixed to the beamline. The sample was set to an incidence angle of 30° (between the normal surface vector and incident beam). The XANES measurements were performed on the SGM beamline at the Canadian Light Source (Saskatoon, SK, Canada)[24]. The XANES measurements were recorded in total fluorescence yield (TFY) mode with a high voltage channel plate detector with the sample surface perpendicular to the incident beam. The XANES measurements were normalized during the experiment using the photocurrent from a highly transparent gold mesh to monitor changes in the incident photon flux. XES and XANES spectra were energy-calibrated using the reference compounds h-BN and BGO (bismuth germanate), and the energy locations of the spectra used were the same as those in Ref. 25.

The sample synthesis and structural characterization proceeded similarly to that described in Ref. 14 and as such the structural parameters described therein were used to create the structural models presented here. The structural models (see Table I), #1 - 3, were created using the lattice parameters and fractional coordinates found in Ref. 14. In the refinement of the spinel-type structured gallium-oxonitride within the space group $Fd\bar{3}m$, all of the anions and vacancies are placed on the Wyckoff position 32e possessing an F symmetry, and as such an ordering of the anions would lead to a reduction of the symmetry. Three different space groups were identified, in which an ordering of the anions could be described. It is important to note that these structures only differ by the placement of the N and O atoms in the anion sites. If the N and O were indistinguishable, the space group would revert back to $Fd\bar{3}m$. The N/O ratio was a 2:6 occupation of the 8 available anionic sites in the F lattice. Contrarily, the structure determination of a single-crystal (Ref. 14) showed vacancy rates of 7% (cation) and 5% (anion), but were not included in the model structures used herein as they would not contribute significantly to the experimental measurements due to the limited available resolution, and therefore would not affect any comparison to the experimental data (but would increase the complexity of the calculations significantly).

The software package WIEN2k was used for all DFT calculations[26]. The exchange correlation functionals used were the generalized gradient approximation of Perdew-Burke-Ernzerhof (PDE)[27] and the LDA functional including the semi-local potential modified from that of

Becke and Johnson (MBJLDA)[20]. A 12 × 12× k-point mesh was employed for a unit cell with plane wave energy cut off of -6.0 Rydberg and a R_kmax of 7.0. The sphere sizes used to enclose the core electron wave functions were 2.000, 1.5600, and 1.5600 Bohr for Ga, N, and O, respectively. A 1 × 2 × 1 supercell incorporating a full core hole was used to simulate the XANES, and the k-point mesh was reduced to 8 × 4 × 8. Four important aspects need to be taken into account when comparing XES and XANES measurements directly to theoretical LPDOS calculations. These are final state considerations, lifetime broadening, instrumental broadening, and non-equivalent site contributions. Further details pertaining to simulating XANES and XES with this method is described elsewhere in detail[15,25].

TABLE I. The structural details of all crystal structures used in this study are listed. Please note, the fractional coordinates for structure #3 are given in rhombohedral coordinates and the lattice parameters are given using hexagonal lattice vectors. All structures were created from the structural details of Ref. 14.

Atom	**Wyck.**	**Frac. *x***	**Frac. *y***	**Frac. *z***
Structure #1				
Ga1	4*a*	1/2	0	3/4
Ga2	4*b*	3/4	3/8	3/4
Ga3	4*b*	1/4	1/4	0
N	4*b*	1/4	0.0069	0.5138
O1	4*b*	1/4	0.4931	0.4862
O2	8*c*	0.4862	0.2569	1/4
Structure #2				
Ga1	2*a*	0	0	0
Ga2	2*b*	0	1/2	1/4
Ga3	4*c*	3/4	0	3/8
Ga4	4*d*	0	1/4	5/8
N	4*c*	0.2638	0	0.1319
O1	4*c*	0.7638	0	0.6181
O2	4*d*	0	0.7638	0.3819
O3	4*d*	0	0.7362	0.8681
Structure #3				
Ga1	1*a*	0	0	0
Ga2	2*c*	0.3750	0.3750	0.3750
Ga3	3*d*	1/2	0	0
N	2*c*	0.2431	0.2431	0.2431
O	6*h*	0.2431	0.2431	0.7707

Structure #1 *Ima*2 (No. 46): a,c = 5.8534 Å b = 8.2780 Å
Structure #2 *Imm*2 (No. 44): a,b = 5.8534 Å c = 8.2780 Å
Structure #3 $R\bar{3}m$ (No. 166): a,b = 5.8534 Å c = 14.3379 Å

The band gap or energy gap of a material is the difference in energy between the highest occupied DOS (or the top of the VB probed by XES) and the lowest unoccupied DOS (or the bottom of the CB probed by XANES). The band gap can therefore be determined by combining XES and XANES measurements on a common energy scale. There are three important experimental effects that need to be accounted for when using SXS to determine the band gap. Core hole effects can shift the CB states to lower energies, effectively decreasing the measured band gap. Non-equivalent sites will have different core level binding energies resulting in splitting of the spectral contributions and effectively decreases the measured band gap. The VB and CB are affected by experimental broadening and the VB and CB locations are determined using the second derivative of the corresponding spectrum[28]. These three corrections help provide more reliable and accurate band gap estimates.

III. RESULTS AND DISCUSSION

A. Anion Ordering

The anion ordering in spinel-type gallium oxonitride is a pertinent question. Ascertaining the exact nature of the bonding allows for further study of the electronic and mechanical properties. As mentioned previously, each unique crystal structure produces a unique electronic structure. While we cannot directly measure the local anion ordering (the location of the N and O atoms), we can probe the electronic structure and indirectly determine the specific location of the anion atoms.

Figure 1 shows a comparison of the measured and simulated O 1*s* XANES spectra, which suggest that structure #3 exhibits the most proper anion ordering. The unoccupied O *p*-states have three features labelled d', e' and f', but only two features, d' and e' change throughout the different structures. The measured unoccupied O *p*-states suggest that the relative intensity of these features, d' and e', should be approximately the same. The origin of these features may be elucidated with the partial density of states (PDOS). Figure 2 shows the PDOS for structures #1, 2 and 3, and are used to look at the detailed electronic structure information since simulated the XES and XANES spectra require significant broadening resulting in a loss of detail. Here, the PDOS clearly show that feature d' is attributed to Ga *s* — O *p* hybridization, while feature e' is attributed to Ga *p* — O *p* hybridization. Examining Fig. 1, we see that of the structures #1-3, #3 has the largest amount of Ga *p* — O *p* hybridization and best reproduces the measured unoccupied O *p*-states.

Figure 1 also shows a comparison of the measured and simulated O K_α XES spectra, which also suggest that structure #3 has the most appropriate anion ordering. The simulated occupied O *p*-states have a similar shape between the different structures. There is however, one key distinguishing feature, which is the prevalence of occupied O *p*-states near the Fermi Level (feature c'). The origin of this effect is explained by examining the calculated unbroadened PDOS. The occupied O *p*-states near the Fermi level change significantly between structural

models. The difference in c' between the different structures is that in structures #1 and 2, the occupied O p-states are withdrawn from the Fermi level and do not contribute the top of the VB. This is contrary to structure #3 in which the occupied O p-states do contribute the top of the VB. Now in the measured O K_α XES spectra, the O p-states contribute largely to the top of the VB best corresponding to the occupied O p-states of structure #3, which is the only model where the occupied O p-states are at the top of the VB. This small, but definite difference, suggests structure #3 is the appropriate structure since the measurements suggest that O p-states do contribute to the top of the VB. This suggests the structure #3 is the most appropriate model for $Ga_{2.79}O_{3.05}N_{0.76}$ compound studied here.

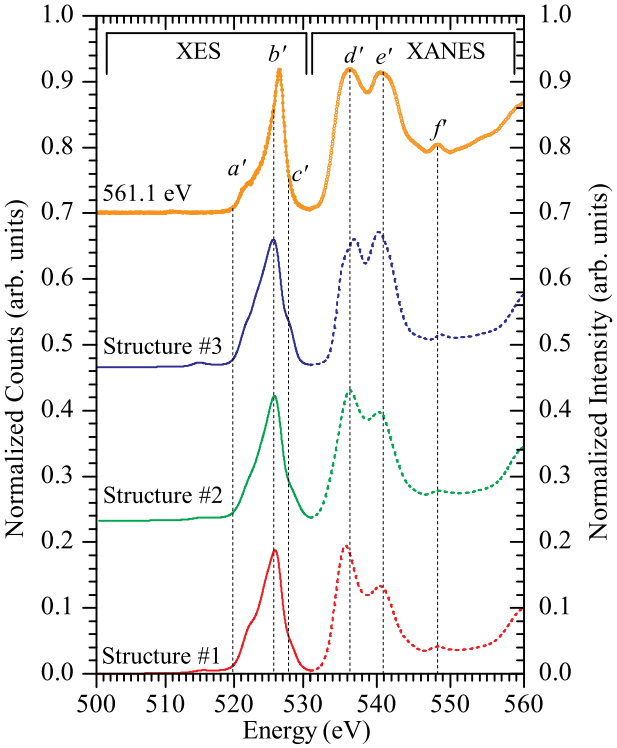

FIG. 1. The measured (scatter) and simulated (solid and dashed lines) O K_α XES and O 1s XANES spectra probe the occupied and unoccupied O p-states, respectively. A comparison of the simulated and measured data determines which structural model best reproduces the experiment. Vertical dashed lines indicate spectral features and are used to guide the eye to the comparable features of the simulated and measured spectra. The annotation to the left of the spectrum indicates the corresponding structural model outlined in Table I or the excitation energy of the measured O K_α XES spectra.

Figure 3 shows a comparison of the measured and simulated N 1s XANES spectra, which further elucidates the appropriate anion ordering, but these measurements are contaminated with remaining h-BN that was used as the crucible material during the synthesis of $Ga_{2.79}O_{3.05}N_{0.76}$. We therefore need to take into account the effect the h-BN impurity will have on the measured N p-states making it not readily apparent which structural model best reproduces the measured N p-states. The measured unoccupied N p-states of $Ga_{2.79}O_{3.05}N_{0.76}$ bear a striking resemblance to that of h-BN unoccupied N p-states, but with a few subtle differences. These differences are: the relative intensity ratio of the features f/h is smaller for h-BN and the unoccupied N p-states of $Ga_{2.79}O_{3.05}N_{0.76}$ extend lower in energy indicating a smaller band gap than h-BN, which we expect from theoretical calculations presented here. With a difference in the intensity of features f and h in mind, we would expect that for our simulated unoccupied N p-states the relative intensity ratio of f/h would be larger than the measured $Ga_{2.79}O_{3.05}N_{0.76}$, since the addition of an h-BN spectrum will reduce the relative intensity.

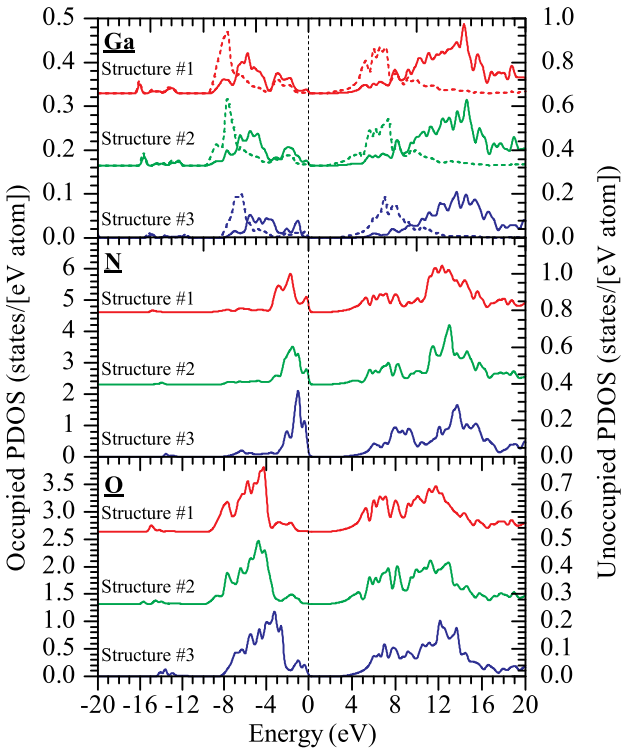

FIG. 2. The partial densities of states (PDOS) of Ga_3O_3N including Ga s-states (dashed) and Ga/N/O p-states (solid) for structures #1, #2 and #3 are displayed in red, blue and green, respectively. The PDOS has been broadened to allow for easy comparisons. The top of the valence band (VB) is set to 0.0 eV and is indicated with a vertical dashed line. The colours of the PDOS correspond to a specific structural model in the same scheme as figures 1 and 3.

This ratio again can be correlated to the electronic structure and Figure 2 shows the PDOS for the unoccupied N p-states. These figures show that feature f is a result of N p — Ga s hybridization and feature h is due to N p — Ga p hybridization. The unoccupied N p-states pertaining structure #3 have the largest rela-

tive intensity ratio of these features suggesting that it is the appropriate structural model for $Ga_{2.79}O_{3.05}N_{0.76}$. While, the reduced band gap of $Ga_{2.79}O_{3.05}N_{0.76}$ is not useful for the comparison of the unoccupied N p-states it does prove fruitful in the comparison of the occupied N p-states.

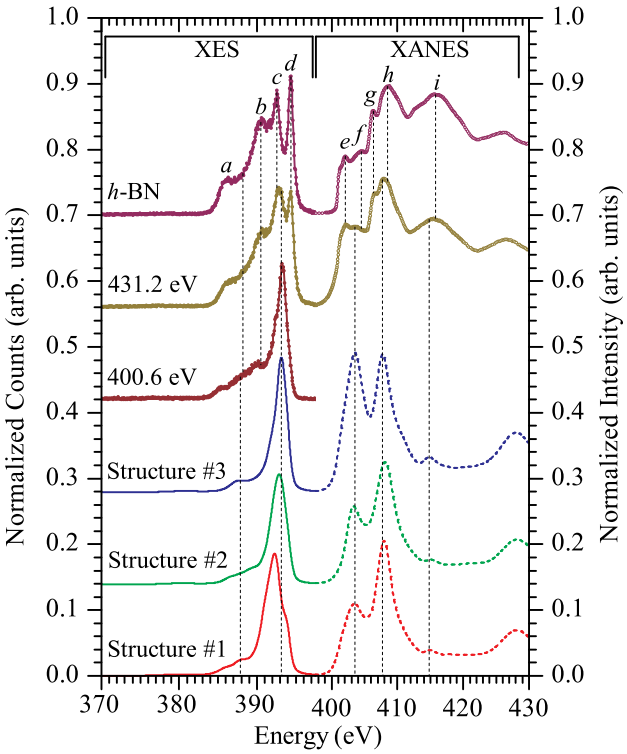

FIG. 3. The measured (scatter) and simulated (solid and dashed lines) N K_α XES and N 1s XANES spectra probe the occupied and unoccupied N p-states, respectively. A comparison of the simulated and measured data determines which structural model best reproduces the experiment. Vertical dashed lines indicate spectral features and are used to guide the eye to the comparable features of the simulated and measured spectra. The annotation to the left of the spectrum indicates the corresponding structural model outlined in Table I or the excitation energy of the measured N K_α XES spectra.

Figure 3 also shows a comparison of the measured and simulated N K_α XES spectra, which confirm that the anion ordering in Structure #3 best reproduces the measured occupied N p-states. The band gap difference of $Ga_{2.79}O_{3.05}N_{0.76}$ in comparison to h-BN allows us to tune the XES spectrum excitation energy to the lowest value possible in order to avoid photons being absorbed by h-BN. Thus, we predominantly probe the occupied N p-states of the $Ga_{2.79}O_{3.05}N_{0.76}$ present in the sample as opposed both h-BN and $Ga_{2.79}O_{3.05}N_{0.76}$. The corresponding XES spectrum is labelled as 400.6 eV in Fig. 3. The measured occupied N p-states change drastically and look almost identical to those calculated for structure #3, confirming our previous conclusion drawn from the comparison of the measured and simulated unoccupied N p-states. This confirms the appropriate structure is #3.

So far, structure #3 is determined to provide the most correct model of the anion ordering out of the three structures tested. This is largely based on the nature of bond hybridization that is seen in the experimental measurements. The cause of this large degree of hybridization of the Ga-O and Ga-N bonds may be due to the highly symmetry of the bonding polyhedra, see Figure 4. As discussed earlier, the nitrogen atoms substitute such that they increase the separation as much as possible, however, the increased stability may be due to the symmetry of the polyhedra that occurs. This is not uncommon for spinel structure compounds, for example, in the solid solutions γ-$(Si,Ge)_3N_4$ Ge occupies the tetrahedral sites because it allows the most symmetric N-(Ge,Si) tetrahedra to exist[8,9]. With the notion that the anions would be prefer to be distributed as symmetrically as possible in bonding polyhedra, it seems unlikely that a random distribution of anions would achieve better results.

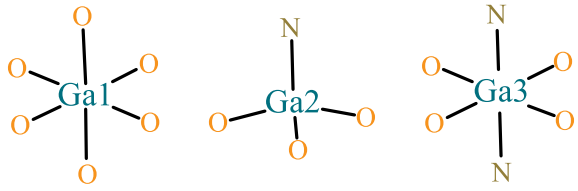

FIG. 4. The bonding polyhedra of structure #3 are Ga-O_6 (left), Ga-O_3N (center) and Ga-O_4N_2 (right). These highly symmetric polyhedra represent the local bonding environment that is responsible for the bond hybridization.

B. Electronic Band Gap

Now that we have determined the most probable model for the anion ordering to be structure #3, we turn our attention to the electronic band gap of $Ga_{2.79}O_{3.05}N_{0.76}$. The measured oxygen data are not affected by h-BN impurities and are used to evaluate the electronic band gap.

The band gap is determined by combining the measured occupied and unoccupied O p-states on the same energy scale as in Fig. 1. Figure 5 displays the second derivative of the measured occupied and unoccupied O p-states and is used to determine the location of the VB and CB edges. There is no significant core hole shift (0.0 $\pm$ 0.1 eV) as determined from our DFT calculations by comparing the calculations with and without a core hole. This places the measured band gap of $Ga_{2.79}O_{3.05}N_{0.76}$ at 2.95 $\pm$ 0.30 eV with no corrections necessary since there is only one oxygen site in structure #3. The error associated with this band gap value is evaluated by including three considerations: the error in the experimental precision in energy ($\pm$ 0.20 eV), the error in the

relative calibration (± 0.20 eV) and the error in the core-hole shift (± 0.1 eV).

The electronic band gap values were also implicitly calculated from the DFT calculations. Table II lists both the band gap values calculated with PBE and MBJLDA. It is well known that conventional GGA(PBE) calculations underestimate the band gap, but including a semi-local screening potential provides significantly more accurate values[20]. The calculated band gap values for structure #3 are used as the theoretical values for $Ga_{2.79}O_{3.05}N_{0.76}$. The reliability of MBJLDA band gap calculations of similar compounds, w-GaN and β-Ga_2O_3, suggests that the value should be within 0.2 eV, which is what we see when we compare the calculated value and the measured value.

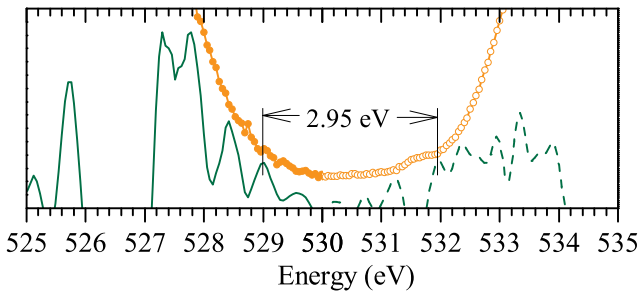

FIG. 5. The second derivatives (solid and dashed) of the measured (scatter) non-resonant O K_α XES and O 1s XANES spectra determine the top of the VB and bottom of the CB. The first peak above the background noise level is used to determine the VB and CB edges.

IV. CONCLUSIONS

Here we tested three structural models for Ga_3O_3N in which there is a significant level anion ordering, contrary to XRD diffraction measurements, which generalize the anions to a single site. We confirm that of the three possible structure types tested, the appropriate structural model is that which adopts the $R\bar{3}m$ space group. This structure provides the appropriate hybridization of Ga s and p — N and O p states. The high level of hybridization stems from the increased symmetry of the Ga-O_6/Ga-O_4N_2 octahedra and Ga-O_3N tetrahedra. The measured band gap of $Ga_{2.79}O_{3.05}N_{0.76}$ is 2.95 ± 0.30 eV using the O K_α XES and O 1s XANES spectra, and agrees with the calculated value of 2.79 eV. We use a combination of DFT calculations along with XES and XANES measurements to experimentally determine both the band gap and anion ordering in spinel-type gallium oxonitride for the first time. This technique is not limited to this material but may applied to any material where the locations of the elements, differing by $\Delta Z \pm 1$, are not easily determined with XRD.

TABLE II. The calculated band gap values using PDE (E-g^{PDE}) and MBJLDA (E_g^{MBJLDA}) are compared to the experimentally determined value (E_g^{exp}). The type of band gap transition that can occurs is indicated in parenthesis. The calculated band gap values using the same method for w-GaN and β-Ga_2O_3 illustrate the reliability of the calculated values.

Material	$\mathbf{E}_g^{PBE}$ (eV)	$\mathbf{E}_g^{MBJLDA}$ (eV)	$\mathbf{E}_g^{Exp.}$ (eV)
$Ga_{2.79}O_{3.05}N_{0.76}$	1.14 (direct)	2.79 (direct)	2.95 ± 0.30
w-GaN	1.94	3.23	3.4 ± 0.1
β-Ga_2O_3	2.50	4.96	4.8 ± 0.1

ACKNOWLEDGMENTS

We gratefully acknowledge the Natural Sciences and Engineering Research Council of Canada (NSERC) and the Canada Research Chair program for their support in this research. Research described in this paper was performed at the Canadian Light Source, which is supported by the Natural Sciences and Engineering Research Council of Canada, the National Research Council Canada, the Canadian Institutes of Health Research, the Province of Saskatchewan, Western Economic Diversification Canada, and the University of Saskatchewan.The Advanced Light Source is supported by the Director, Office of Science, Office of Basic Energy Sciences, of the U.S. Department of Energy under Contract No. DE-AC02-05CH11231. The Deutsche Forschungsgemeinschaft financially supported this work (contracts KI 838/3-1 and HU 966/5-1). R. Riedel is grateful to the Fonds der Chemischen Industrie for financial support.

* teak.boyko@usask.ca

[1] A. Zerr, G. Miehe, G. Serghiou, M. Schwarz, E. Kroke, R. Riedel, H. Fuess, P. Kroll, and R. Boehler, Nature **400**, 340 (1999).

[2] G. Serghiou, G. Miehe, O. Tschauner, A. Zerr, and R. Boehler, J. Chem. Phys. **111**, 4659 (1999).

[3] T. Sekine, H. L. He, T. Kobayashi, M. Zhang, and F. F. Xu, Appl. Phys. Lett. **76**, 3706 (2000).

[4] K. Leinenweber, M. O'Keeffe, M. Somayazulu, H. Hubert, P. F. McMillan, and G. H. Wolf, Chem. -Eur. J. **5**, 3076 (1999).

[5] M. Schwarz, G. Miehe, A. Zerr, E. Kroke, B. Poe, H. Fuess, and R. Riedel, Adv. Mater. **12**, 883 (2000).

[6] W. Y. Ching, S.-D. Mo, I. Tanaka, and M. Yoshiya, Phys. Rev. B **63**, 064102 (2001).

[7] W. Y. Ching, S. D. Mo, and L. Ouyang, Phys. Rev. B **63**, 245110 (2001).

[8] J. Dong, J. Deslippe, O. F. Sankey, E. Soignard, and P. F. McMillan, Phys. Rev. B **67**, 094104 (2003).

[9] E. Soignard, P. F. McMillan, and K. Leinenweber, Chem. Mater. **16**, 5344 (2004).

[10] P. Kroll, R. Dronskowski, and M. Martin, J. Mater. Chem. **15**, 3296 (2005).

[11] P. Kroll, Phys. Rev. B **72**, 144407 (2005).

[12] E. Soignard, D. Machon, P. F. McMillan, J. J. Dong, B. Xu, and K. Leinenweber, Chem. Mater. **17**, 5465 (2005).

[13] O. U. Okeke and J. E. Lowther, Phys. Rev. B **77**, 094129 (2008).

[14] H. Huppertz, S. A. Hering, C. E. Zvoriste, S. Lauterbach, O. Oeckler, R. Riedel, and I. Kinski, Chem. Mater. **21**, 2101 (2009).

[15] T. D. Boyko, E. Bailey, A. Moewes, and P. F. McMillan, Phys. Rev. B **81**, 155207 (2010).

[16] J. E. Lowther, T. Wagner, I. Kinski, and R. Riedel, J. Alloy. Compd. **376**, 1 (2004).

[17] I. Kinski, G. Miehe, G. Heymann, R. Theissmann, R. Riedel, and H. Huppertz, Z. Naturforsch. (B) **60**, 831 (2005).

[18] W. Y. Ching and P. Rulis, Phys. Rev. B **73**, 045202 (2006).

[19] Y. N. Xu and W. Y. Ching, Phys. Rev. B **51**, 17379 (1995).

[20] F. Tran and P. Blaha, Phys. Rev. Lett. **102**, 226401 (2009).

[21] E. Soignard, P. F. McMillan, C. Hejny, and K. Leinenweber, J. Solid State Chem. **177**, 299 (2004).

[22] K. Tatsumi, T. Mizoguchi, S. Yoshioka, T. Yamamoto, T. Suga, T. Sekine, and I. Tanaka, Phys. Rev. B **71**, 033202 (2005).

[23] J. J. Jia, T. A. Callcott, J. Yurkas, A. W. Ellis, F. J. Himpsel, M. G. Samant, J. Stöhr, D. L. Ederer, J. A. Carlisle, E. A. Hudson, L. J. Terminello, D. K. Shuh, and R. C. C. Perera, Rev. Sci. Instrum. **66**, 1394 (1995).

[24] T. Regier, J. Krochak, T. K. Sham, Y. F. Hu, J. Thompson, and R. I. R. Blyth, Nucl. Instrum. Methods Phys. Res. Sect. A-Accel. Spectrom. Dect. Assoc. Equip. **582**, 93 (2007).

[25] C. Braun, M. Seibald, S. L. Boerger, O. Oeckler, T. D. Boyko, A. Moewes, G. Miehe, A. Tuecks, and W. Schnick, Chem. -Eur. J. **16**, 9646 (2010).

[26] K. Schwarz, P. Blaha, and G. K. H. Madsen, Comp. Phys. Comm. **147**, 71 (2002).

[27] J. P. Perdew, K. Burke, and M. Ernzerhof, Phys. Rev. Lett. **77**, 3865 (1996).

[28] E. Z. Kurmaev, R. G. Wilks, A. Moewes, L. D. Finkelstein, S. N. Shamin, and J. Kuneš, Phys. Rev. B **77**, 165127 (2008).